Journal of Materials Chemistry A

Accepted Manuscript

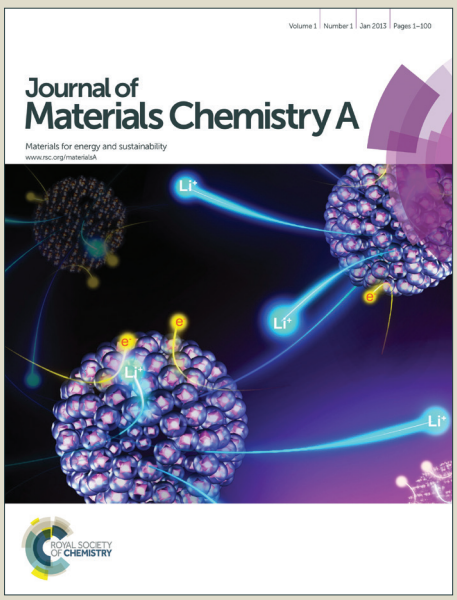

ROYAL SOCIETY OF CHEMISTRY

www.rsc.org/materialsA

Journal Name

RSCPublishing

ARTICLE

Highly sensitive and selective fluorescent probe for Ag^+ based on a Eu^{3+} post-functionalized metal-organic framework in aqueous media

Cite this: DOI: 10.1039/x0xx00000x

Received 00th January 2012,
Accepted 00th January 2012

DOI: 10.1039/x0xx00000x

www.rsc.org/

Ji-Na Hao, Bing Yan*

A 3D microporous compound $Al(OH)(H_2btec)\cdot H_2O$ (MIL-121) containing uncoordinated carbonyl groups is chosen as a parent metal-organic framework (MOF). And because the uncoordinated carbonyl groups in the channels could act as postsynthetic modification sites, a robust luminescent lanthanide-based MOF can be constructed by encapsulating Eu^{3+} cations into the pores of MIL-121. The intense luminescence of Eu^{3+} incorporated MIL-121 products demonstrates that the framework with rigid, permanently porous structure and non-coordinated carboxyl group is an efficient scaffold for hosting and sensitizing Eu^{3+} cations. More significantly, the robust Eu^{3+}@MIL-121 shows excellent selectivity, fast detection time (< 5 min), and high sensitivity (detection limit, 0.1 μM) for Ag^+ ions in aqueous solution through greatly enhancing of the Eu^{3+}-luminescence. This is a rare example to detect Ag^+ in aqueous solutions based on a luminescent lanthanide MOFs.

Introduction

As heavy metal ions can cause severe risks for the environment and human health, metal ion sensing and detection are significant in life sciences, environmental science, medicine science and nuclear industry.[1] Due to human activities, the Ag^+ content in the vicinities of sewage outfalls, electroplating plants, mine waste sites, and silver-iodide seeded areas has increased. Ag^+ can accumulate in the human body through the food chain and drinking water. What's more, silver ions are known to bind with various metabolites, including amine, imidazole, and carboxyl groups, and inactivate sulfhydryl enzymes,[2] Therefore, the deficiency of Ag^+ will result in a number of pathological disorders, such as cell toxicity and organ failure. Thus, it is of considerable importance for the environment and human health to establish an Ag^+ detection method with high sensitivity and high selectivity. At present, among the detection methods, fluorometric methods have gained much attention due to their distinct advantages, i.e. facilitated detection and manipulation and high sensitivity.[3] Meanwhile, there is an urgent need to develop fluorescent chemosensors that are capable of determining of silver ions in various media.

Metal-organic frameworks (MOFs), a class of crystalline hybrid inorganic-organic materials constructed from organic linker molecules and metal ions, have shown a variety of potential applications, such as gas adsorption,[4] separations,[5] catalysis,[6] and sensing.[7] Particularly, among the diverse MOFs, those displaying interesting luminescence properties are receiving increasing attentions because they are useful for the development of sensing technologies.[8] Of particular interest are lanthanide metal-organic frameworks (Ln-MOFs) since their fascinating optical properties[9], such as large Stokes' shifts, high color purity, and relatively long luminescence lifetimes, make them especially attractive for sensing applications.[10] In the past decade, studies on luminescent Ln-MOFs for sensing metal ions or organic molecules have been developed significantly. Such progress in the sensing application of Ln-MOFs guides and inspires us to rationally design and synthesize Ln-MOFs for host-guest recognition and to tune their functional properties. However, rational design and preparation of the desired Ln-MOFs still remain a great challenge,[11] which is obviously because Ln^{3+} ions have higher coordination numbers and more variable nature of the Ln coordination sphere, and the open lanthanide sites formed in situ during activation/de-solvation tend to bind back with the oxygen/nitrogen donors from the organic linker to form a condensed structure. Nonetheless, the above problems did not deter researchers from exploring the luminescent lanthanide-containing MOFs. Recently, an alternative strategy to construct lanthanide-based MOFs is by postsynthetic method (PSM)[12] whose chemical modification can be performed on the fabricated material rather than on the molecule precursors. This provides a new choice for building lanthanide MOFs. An increasing number of Ln-doped MOFs constructed by PSM have been made in recent years. This is the case for bio-MOF-1,[13] Zn(II)-MOF,[14] COMOC-4,[15] MOF-COOH,[16] Al-MIL-53-COOH.[17] Stimulated by this, herein a lanthanide doped MOFs was prepared by PSM and developed as the luminescent sensor.

In this context, as a MIL-53(Al) analogue, MIL-121 (aluminium pyromellitate or $Al(OH)(H_2btec)\cdot H_2O$, H_4btec= pyromellitic acid), which contains two extra free carboxylic acid functions per ligand with interesting porosity,[18] was chosen as a parent framework. The reactive nature of the uncoordinated carbonyl

groups as well as the high thermal and chemical stabilities of MIL-121 makes it a good candidate to bind Ln^{3+} cations. As a result, a new class of lanthanide luminescent MOFs was generated by encapsulating Eu^{3+} into MIL-121 crystals. The high luminescence of Eu^{3+} incorporated MIL-121 products (Eu^{3+}@MIL-121) demonstrated that the framework with rigid, permanently porous structure and non-coordinated carboxyl was an efficient scaffold for hosting and sensitizing Eu^{3+} cations. More significantly, the Eu^{3+}@MIL-121 was developed as highly selective and sensitive fluorescence probe targeting Ag^{+} ions in aqueous solutions, which could be proved by the fact that Eu^{3+}@MIL-121 exhibits an impressive enhancing phenomenon upon the typical Eu-luminescence in the case of Ag^{+} ions. Although considerable efforts have been devoted for the development of fluorescent chemosensors specific for cations, there are only a handful of reports on molecular probes for Ag^{+} ions and, to the best of our knowledge, there are fewer reports about the Ag^{+} optical sensor based on the lanthanide luminescence MOFs.

Experimental section

Materials and instrumentation. The salts of $LnCl_3 \cdot 6H_2O$ were prepared by dissolving the corresponding lanthanide oxide compounds in excess hydrochloric acid (37 %) followed by evaporation and crystallization. pyromellitic acid (98 %) was purchased from Adamas and used directly without further purification. All the other starting materials and reagents were all AR and used as purchased. The crystalline phases of the products were determined by X-ray powder diffraction patterns (XRD) using a Rigaku D/max-Rb diffractometer equipped with Cu anode. Fourier transform infrared spectra (FTIR) were recorded with a Nexus 912 AO446 infrared spectrum radiometer within the wavenumber range 4000 – 400 cm^{-1} using the KBr pressed technique. Excitation and emission spectra of the solid samples were obtained on Edinburgh FLS920 spectrophotometer. Thermogravimetric analysis (TG) was measured using a Netzsch STA 449C system at a heating rate of 5 K min^{-1} under the nitrogen protection. Luminescence lifetime measurements were carried out on an Edinburgh FLS920 phosphorimeter using a 450 W xenon lamp as excitation source. The outer absolute luminescent quantum efficiency was determined using an integrating sphere (150 mm diameter, $BaSO_4$ coating) from an Edinburgh FLS920 phosphorimeter. The quantum yield can be defined as the integrated intensity of the luminescence signal divided by the integrated intensity of the absorption signal. The absorption intensity was calculated by subtracting the integrated intensity of the light source with the sample in the integrating sphere from the integrated intensity of the light source with a blank sample in the integrating sphere.

Synthetic Procedures.

Typical synthesis of MIL-121. The compound MIL-121 was prepared by hydrothermal reaction of $Al(NO_3)_3 \cdot 9H_2O$ (1.2 g, 3.2 mmol) and pyromellitic acid (noted H_4btec, 0.4 g, 1.6 mmol) in 5 mL of deionized water at 210 °C for 24 hrs. The starting pH value was 1.41 and 0.26 at the end of the reaction. It resulted in a white powdered product, which was filtered off, washed with deionized water, and dried at 80 °C for 12 hrs in vacuum.[18] To remove the organic species encapsulated within the pores of the open framework, the samples were activated by Soxhlet extraction in methanol for 24 h and then dried at 80 °C under vacuum overnight.

Eu^{3+}@MIL-121 Preparation. Eu^{3+}@MIL-121 was prepared by stirring the mixture of 100 mg of MIL-121 and 2 mmol $EuCl_3 \cdot 6H_2O$ in 10 mL ethanol at 60 °C for 48 hrs. The solid was then separated from the mixed dispersion by centrifugation, and extensively washed with ethanol to remove residual Eu^{3+} cations on the surface. Subsequently, the resulted white powder was dried under vacuum at 80 °C for 12 hrs.

Luminescence-sensing experiment. 3 mg of Eu@MIL-121 were simply immersed in the aqueous solutions of $M(NO_3)_z$ (10^{-2} mol·L^{-1}, 3 mL) at room temperature (M^{z+} = Na^{+}, K^{+}, Mg^{2+}, Ca^{2+}, Al^{3+}, Cr^{3+}, Mn^{2+}, Fe^{3+}, Co^{2+}, Ni^{2+}, Cu^{2+}, Ag^{+}, Zn^{2+}, Cd^{2+}, Hg^{2+}, Pb^{2+}).[7a,10a] The mixtures were then sonicated for 30 min to form the metal ion-incorporated suspension for luminescent measurements.

Results and discussion

Characterization of Eu^{3+}@MIL-121

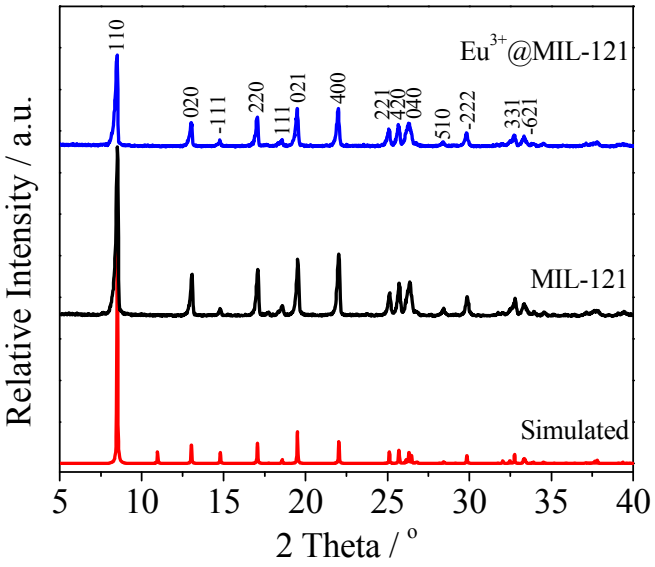

Figure 1 PXRD of MIL-121 (black line) and Eu^{3+}@MIL-121 (blue line).

The compound MIL-121 was solvothermally synthesized by mixing aluminum nitrate, pyromellitic acid, and H_2O. The powder XRD pattern of the resulted product (Figure 1) agrees well with the literature value.[18] The MIL-121 is a three-dimensional (3D) framework containing one-dimensional (1D) channels delimited by infinite trans-connected aluminum-centered octahedral $AlO_4(OH)_2$ linked through the pyromellitate ligand. Here only two carboxylate arms of the pyromellitate play the role of linker while the two others remain non-bonded in their protonated form. The non-coordinated –COOH groups points toward the channels to get them an open form configuration. The free –COOH can be found in the IR spectrum of MIL-121 (Figure S1). The bands at 3015, 2659, and 2528 cm^{-1} are assigned to the υ_{CO-H} modes of free –COOH functions. In the range of 1600 − 1800 cm^{-1}, we can differentiate the non-bonded –COOH groups and those connected to aluminum. The peak at 1600 cm^{-1} corresponds to the stretching vibration of carboxylate coordinated to the cation, whereas the vibrations at 1737 and 1716 cm^{-1} are

assigned to non-coordinated functions.[18] This structure was postfunctionalized with a solution of europium (III) chloride in ethanol. The Eu^{3+}@MIL-121 could be formed by the coordination interactions between the free –COOH of MIL-121 and the Eu^{3+} ions. As shown in Figure S2, the absorption band of MIL-121 shows a significant red-shift (~13 nm) after binding to Eu^{3+} ions. This indicates the formation of coordination bonds between the Eu^{3+} ions and free –COOH of MIL-121.[15] After encapsulating Eu^{3+} cations into MIL-121, the material retains its crystallinity well as evidenced by the powder XRD pattern (Figure 1), and the same XRD pattern of Eu^{3+}@MIL-121 with that of MIL-121 also implies that the Eu^{3+} ions are located in the channels of MIL-121 rather than on its skeleton.

The as-prepared Eu^{3+}@MIL-121 was also monitored by TG analysis and N_2 adsorption-desorption. The TG curve of the MIL-121 in Figure 2a exhibits two events. The first one is the elimination of trapped solvent in the pores (~1.5 wt %). The MIL-121 material is thermally stable up to 400 ^oC, above which the total decomposition of the organic ligand (calc.68.6 %) occurs in two steps. The first weight loss of 10 wt % between 400 and 430 ^oC is due to the departure of two CO_2 molecules from the non-coordinating –COOH groups (calc. 8 %). The second step between 430−560 °C is indicative of the decomposition of the ligand (obs. 53 wt %; calc. 60 %). As for Eu^{3+}@MIL-121, the incorporation of Eu^{3+} cations does not influence the thermostability of the framework. The TGA data demonstrates Eu^{3+}@MIL-121 is thermally stable to 400 ^oC, implying the good thermal stability of Eu^{3+}@MIL-121. The MIL-121 particles maintain their microporosity after guest removal, as demonstrated by N_2 sorption isotherm (Figure 2b) showing the BET surface areas of 173 $m^2\ g^{-1}$. The value, which is in reasonable agreement with the result reported by Christophe Volkringer et al,[18] is much lower than the ones determined for the parent compound MIL-53 (BET: 1140 $m^2\ g^{-1}$).[19] The decrease of the BET surface area could be attributed to the steric hindrance of the free non-coordinated carboxyl groups within the channels, which reduce the access of N_2 molecules. After incorporating Eu^{3+} cations, the Eu^{3+}@MIL-121 shows a reduced BET surface area of 102 $m^2\ g^{-1}$.

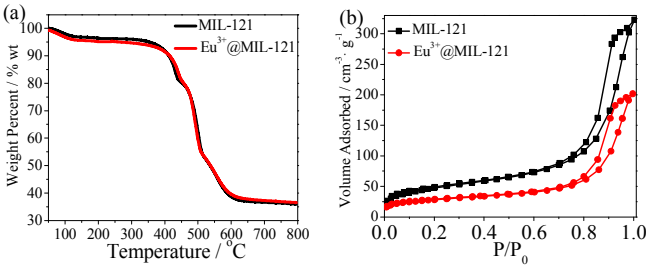

Figure 2 Thermal gravimetric analysis (a) and N_2 adsorption-desorption isotherms (b) of MIL-121 and Eu^{3+}@MIL-121.

Luminescence properties of Eu^{3+}@MIL-121

The room-temperature solid-state photoluminescent emission spectra of the MIL-121 and Eu^{3+}@MIL-121 are shown in Figure S3 and Figure 3, respectively. The MIL-121 displays weak luminescence with a wide band centered around 340 (360) nm when excited by 305 (315) nm. After post-synthetic functionalization of Eu^{3+}, the ligand-centered (LC) emissions are significantly suppressed. Instead, a series of sharp peaks characteristic of Eu^{3+} luminescence appear at 579, 592, 614, 650, and 695 nm, corresponding to the $^5D_0 \rightarrow {}^7F_J$ (J = 0−4) transitions, respectively. The 614 nm emission has maximum intensity, demonstrating that the incorporated Eu^{3+} ions occupy sites without an inversion center and have low crystal field symmetry.[20] This is further confirmed by the presence of 579 nm emission, because this peak only occurs when Eu^{3+} symmetry is low.[15] The diminished LC emission in Eu^{3+}@MIL-121 and the strong red luminescence under UV-light irradiation (inset of Figure 3) indicate that antenna effect occurs, that is, energy migration takes place upon ligand absorption, followed by intersystem crossing $S_1 \rightarrow T_1$ and antenna $T_1 \rightarrow f$ transfer, and then generating f−f emissions of Eu^{3+} ion. Moreover, Eu^{3+}@MIL-121 exhibits reasonable long lifetimes (0.31ms) and quantum yields (6 %), which are attributed to the effective energy transfer from the ligand to the Eu^{3+}. From the above results, we can conclude that MIL-121 can serve as an efficient scaffold for hosting and sensitizing the luminescence of Eu^{3+}.

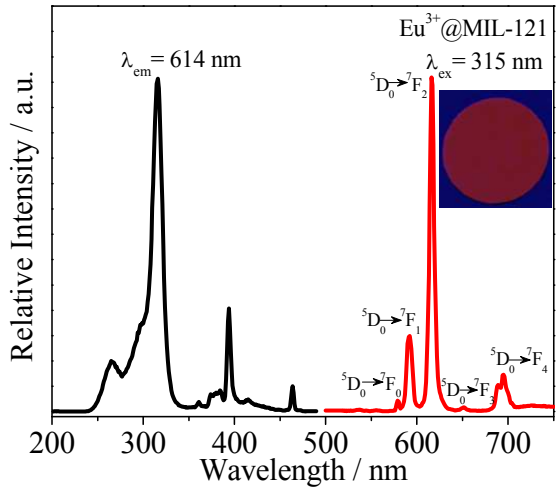

Figure 3 Excitation and emission spectra of Eu^{3+}@MIL-121. The inset is the corresponding luminescence pictures under UV-light irradiation of 254 nm.

The luminescence properties of Eu^{3+}@MIL-121 in aqueous solution have also been investigated in Figure S4. Compared to the solid-state PL spectra of Eu^{3+}@MIL-121, the ligand-centered emission of Eu^{3+}@MIL-121 in aqueous solution cannot be suppressed by the luminescence of Eu^{3+} because of the quenching effect of water molecules. However, the Eu^{3+}@MIL-121 in aqueous solution exhibits excellent fluorescence stability at room temperature. The luminescence intensity of Eu^{3+}@MIL-121 suspension has no obvious change for at least 10 days' storage (Figure S5), implying that Eu^{3+}@MIL-121 possesses great potential as a fluorescence material for sensing in aqueous solution.

Sensing of Ag^+ cations

To examine the potential of Eu^{3+}@MIL-121 for sensing of metal ions, the as-synthesized samples were immersed in the aqueous solutions containing different metal ions (Na^+, K^+, Mg^{2+}, Ca^{2+}, Al^{3+}, Cr^{3+}, Mn^{2+}, Fe^{3+}, Co^{2+}, Ni^{2+}, ,Cu^{2+}, Ag^+, Zn^{2+}, Cd^{2+}, Hg^{2+}, Pb^{2+}) to form the metal ion incorporated MOF suspension for luminescent studies. As shown in Figure 4, various metal ions display markedly different effects on the luminescence of Eu^{3+} ions. For example, the luminescence intensity at 614 nm is decreased when Zn^{2+}, Hg^{2+}, Mn^{2+}, Pb^{2+}, Ni^{2+}, Co^{2+}, Al^{3+}, Cu^{2+}, Cr^{3+}, or Fe^{3+}

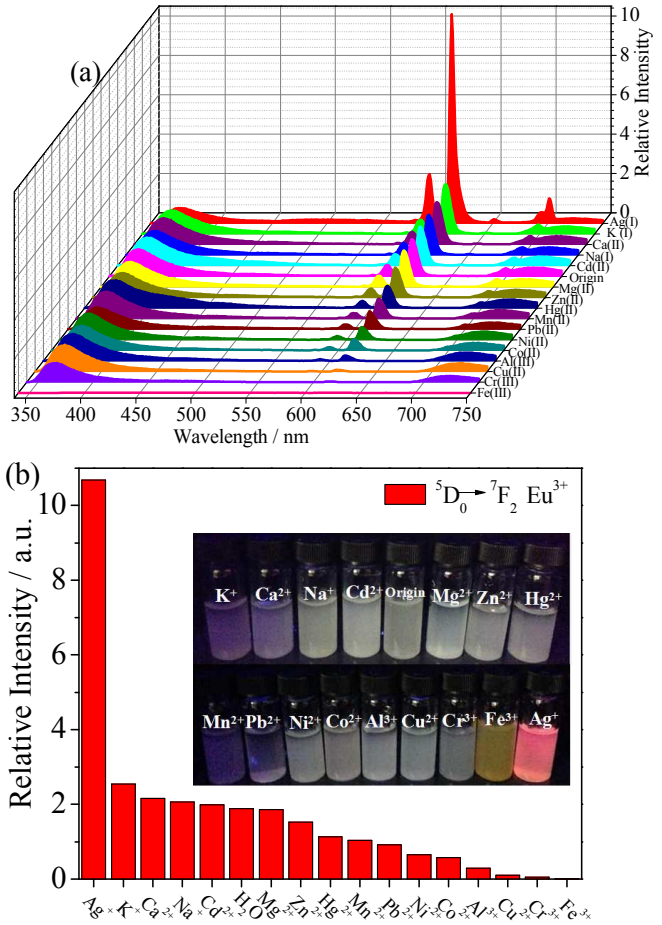

Figure 4 (a) Suspension-state PL spectra and (b) the relative intensities of $^5D_0 \rightarrow {}^7F_2$ at 614 nm for Eu^3+@MIL-121 dispersed in aqueous solutions containing different metal ions (10 mM) when excited at 315 nm. The inset in Figure (b) is the corresponding photographs under UV-light irradiation at 254 nm.

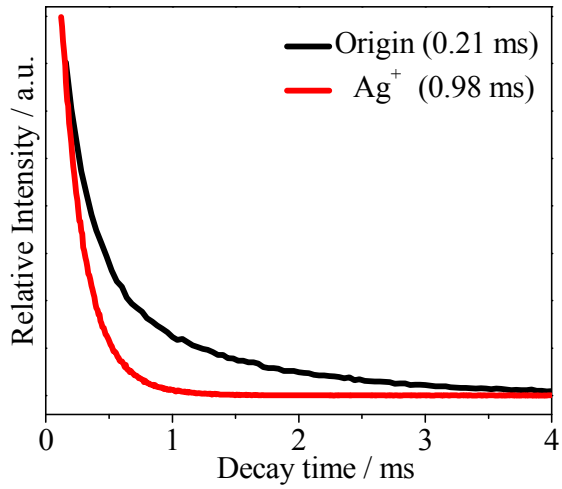

Figure 5 Fluorescence lifetime of Eu^{3+}@MIL-121 in the absence (black) and presence (red) of Ag$^+$ in aqueous solution.

are involved, and Cu^{2+}, Cr^{3+}, or Fe^{3+} can almost quench the luminescence of Eu^{3+}. In contrast, the interaction with Ag^+ drastically enhanced the luminescence intensity, with a maximum of more than 5.0 times as much as that of the original one. The rest of the metal ions (K^+, Ca^{2+}, Na^+, Cd^{2+}, Mg^{2+}) tested did not cause any significant change to the intensity of the luminescence. As a result, only the sample immersed in aqueous solution containing Ag^+ provided direct information of visibly red luminescent color with naked eyes when irradiated under UV light of 254 nm, as shown in the inset of Figure 4b. These results indicate that Eu^{3+}@MIL-121 can selectively sense Ag^+ ions through fluorescence enhancement, which was quite rare in the previous reports on luminescent MOFs. In addition, the enhancement effect of Ag^+ on the luminescence of Eu^{3+}@MIL-121 was evaluated by the fluorescence decay time of Eu^{3+}. Figure 5 shows that the emission lifetimes of Eu^{3+}@MIL-121 significantly increase from 0.21 ms to 0.98 ms in the presence of Ag^+. This observation is in good agreement with the results of PL spectra. The influence of other metal ions on the lifetime of Eu^{3+} was also determined. The lifetime data shown in Table S1 also agree with the responses of luminescence of Eu^{3+}@MIL-121 towards various metal cations.

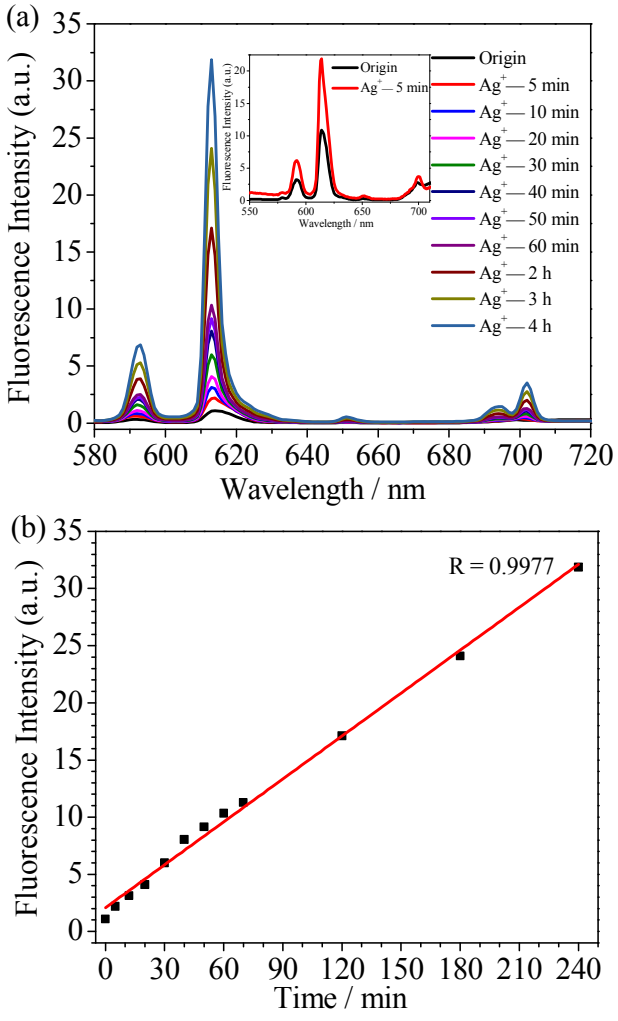

Figure 6 (a) Variation of fluorescence intensity of Eu^{3+}@MIL-121 at 614 nm with immersion time in Ag^+ solution, λ_{ex}=315nm; The inset is the corresponding change of emission intensity when treated with Ag^+ for 5 min. (b) Linear relationship of fluorescence intensity at 614 nm as a function of interaction time.

To investigate the time-response characteristic of the Eu^{3+}@MIL-121 sensor toward Ag^+, the fluorescence intensity of Eu^{3+}@MIL-121 at 614 nm (λ_{ex} = 315 nm) was measured as a

function of immersion time in aqueous solution of 10 mM Ag^+. Figure 6 shows the time-response PL spectra (a) and curves (b) within 4h, respectively. As depicted in Figure 6 (a) and (b), with the interaction time between Ag^+ and Eu^{3+}@MIL-121 increasing, the PL intensity of the sample was continuously enhanced. When the immersing time is 24 hrs, the luminescence intensity reached a constant value (Figure S6). From the inset of Figure 6a, we can see that when the Eu^{3+}@MIL-121 was treated with Ag^+ solution for 5 min, the highest peak at 614 nm was increased to more than 2.0 times as intense as the corresponding band of the original one. This indicates Ag^+-induced fluorescence enhancement reaction is fast.

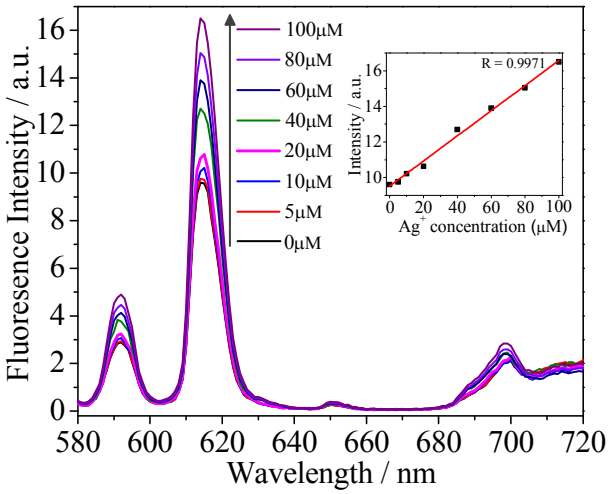

Figure 7 Fluorescence intensity of Eu^{3+}@MIL-121 at 612 nm as a function of Ag^+ concentration in aqueous solution (λ_{ex}=315nm). Insert: linear relationship of Eu^{3+}@MIL-121 enhanced by Ag^+ aqueous solution.

For better understanding the response of fluorescence of Eu^{3+}@MIL-121 to Ag^+, concentration-dependent luminescence measurements were also carried out. The Eu^{3+}@MIL-121 solid samples were immersed in different concentrations of Ag^+ for 24 h, and then their luminescence spectra were recorded. As demonstrated in Figure 7, the emission intensity of Eu^{3+}@MIL-121 suspension enhanced accordingly with the increase of Ag^+ concentration from 0 to 100 μM. In other words, the fluorescence response of Eu^{3+}@MIL-121 toward Ag^+ was linear when measured in the range 0 – 100 μM of Ag^+ (inset of Figure 7). From these data, we have estimated the detection limit of Eu^{3+}@MIL-121 to be 0.1 μM. This detection limit met a 50 μg L^{-1} (about 0.46 μM) standard of U.S. Environmental Protection Agency (EPA) for a maximum allowable level of Ag^+ in drinking water.[21]

In order to make a further understanding of the phenomenon that Ag^+-enhanced the luminescence of Eu^{3+}, the powder XRD was employed to study on the structural data of the Eu^{3+}@MIL-121 and Ag^+/Eu^{3+}@MIL-121 (Figure 8). The powder XRD patterns of the Ag^+/Eu^{3+}@MIL-121 are similar to that of Eu^{3+}@MIL-121, suggesting that the basic frameworks remain unchanged in the compounds, namely, the presence of Ag^+ did not affect the structure of Eu^{3+}@MIL-121. It is well-known that the luminescent intensity of the Ln^{3+} relies on the efficiency of the energy transfer from the ligand to Ln^{3+} center.[22] If there is efficient intramolecular energy transfer, Ln^{3+} can be excited more effectively, producing an enhanced fluorescence of lanthanides. It has been reported that the energy transfer process is more effective with the addition of certain transition metal ions.[23] Herein, we attribute the enhancement of luminescent intensity of Eu^{3+}@MIL-121 to that Ag^+ cause more efficient energy transfer from ligands to Eu^{3+} ions, as depicted in Scheme 1. This is consistent with the results of suspension-state PL spectra of Eu^{3+}@MIL-121 in the absence and presence of Ag^+. Figure S7 shows their excitation spectra monitored by emission wavelength at 614 nm, both of them show the similar broad band

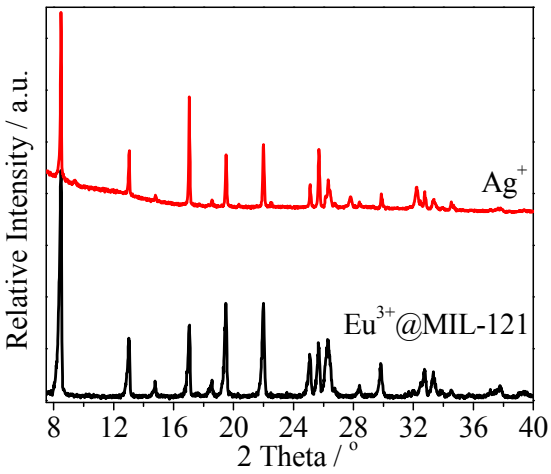

Figure 8 PXRD patterns of the Eu^{3+}@MIL-121 after immersing in aqueous solution with Ag^+ ions.

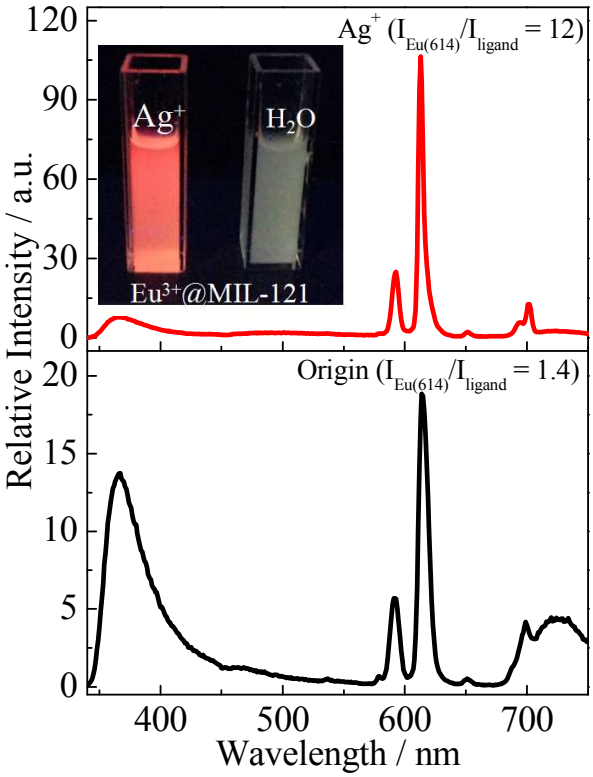

Figure 9 The excitation spectra of Eu^{3+}@MIL-121 in the absence (black) and presence of Ag^+ (red) in aqueous solution. The insert is the corresponding photographs under UV-light irradiation at 254 nm.

centered at 315 nm which can be ascribed to the π→π* electron transitions of the ligands. When excited at 315 nm, the PL emission spectrum (Figure 9a) of the Eu^{3+}@MIL-121 suspension features in observation of two kinds of luminescence. One is the characteristic Eu^{3+} sharp emissions and the other is the broad ligand-centered

emission (370 nm). The absence of the typical intra-configurational transitions of Eu^{3+} in the excitation spectra and the characteristic emissions of Eu^{3+} in the emission spectra corroborate an energy transfer from the organic ligand to the metal ions, but the intense LC emission in the emission spectra indicates that the energy transfer may not of good efficiency (the intensity ratio $I_{Eu(614)}/I_{Ligand}$ of the $^5D_0 \rightarrow {}^7F_2$ line at 614 nm to that of LC emission at 365 nm is 1.4). By contrast, the basically diminished LC emission and the enhanced Eu^{3+}-luminescence of Eu^{3+}@MIL-121 in the presence of Ag^+ (Figure 9b) indicate the energy transfer is more effective ($I_{Eu(614)}/I_{Ligand} = 12$). As a result, with the addition of Ag^+, the fluorescence color of Eu^{3+}@MIL-121 suspension changed from colorless to intense red under a 254 nm UV lamp (inset in Figure 9), which can be easily distinguished by the naked eyes.

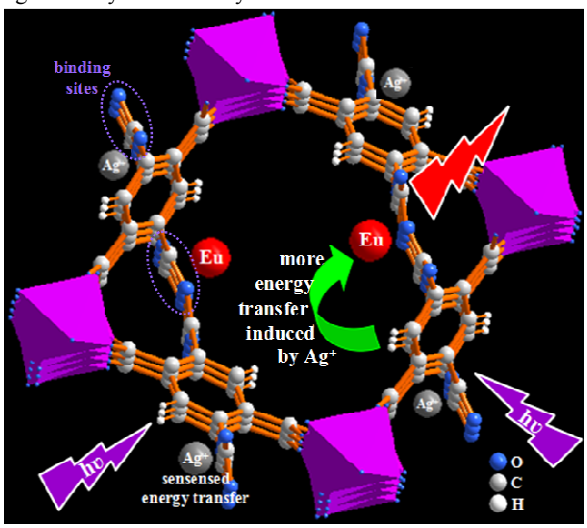

Scheme 1 Illustration of the fluorescence enhancement of Eu^{3+}@MIL-121 by Ag^+.

As luminescent probes, the Eu^{3+}@MIL-121 not only have highly selective and sensitive characteristics but also possesses a stable and robust structure (its frameworks still keeps unchanged in aqueous solution containing various mental ions, shown in Figure S8). It is helpful to extend the potential application of Ln-MOFs to the environment areas.

Conclusions

In summary, a new class of lanthanide luminescent MOFs was generated by postsynthetic modification of encapsulating Eu^{3+} into the pores of MIL-121. The framework with rigid, permanently porous structure and non-coordinated carboxyl could serve as an efficient scaffold for hosting and sensitizing Eu^{3+} cations, demonstrated by the strong luminescence with addition of reasonable lifetimes and quantum yields of Eu^{3+}@MIL-121 products. More significantly, the Eu^{3+}@MIL-121 was performs as a rare example of highly selective and sensitive fluorescence probe for Ag^+ ions in aqueous solutions, which could be proved by the fact that Eu^{3+}@MIL-121 exhibits an impressive enhancing phenomenon upon the typical Eu-luminescence in the case of Ag^+ ions. As a sensing material for Ag^+, Eu^{3+}@MIL-121 has features including simple preparation procedure, robust rigid structure, excellent selectivity, fast detection time (< 5 min), and high sensitivity with a detection limit of 0.1 μM. Although Ag^+-induced luminescence enhancement of Eu^{3+}@MIL-121 was shown, the principle of Ag^+-enhanced fluorescence might be used to improve the fluorescence of other LnMOFs. The related studies are currently under way.

Acknowledgements

This work is supported by the National Natural Science Foundation of China (91122003), the Program for New Century Excellent talents in University (NCET-08-0398) and the Developing Science Funds of Tongji University.

Notes and references

Department of Chemistry, Tongji University, Shanghai 200092, China.
Fax: +86-21-65982287; Tel: +86-21-65984663;
E-mail: byan@tongji.edu.cn

Electronic Supplementary Information (ESI) available: [details of any supplementary information available should be included here]. See DOI: 10.1039/b000000x/

1 (*a*) G. Aragay, J. Pons and A. Merkoci, *Chem. Rev.*, 2011, **111**, 3433; (*b*) D. T. Quang and J. S. Kim, *Chem. Rev.*, 2010, **110**, 6280; (*c*) C. L. Hao, L. G. Xua, C.R. Xing, H. Kuang, L. B. Wang and C. L. Xu, *Biosens. Bioelectron.*, 2012, **36**, 174.
2 (*a*) Q. L. Feng, J. Wu, G. Q. Chen, F. Z. Cui, T. N. Kim and J. O. Kim, *J. Biomed. Mater. Res.*, 2000, **52**, 662; (*b*) A. B. Lansdown, *J. Wound. Care*, 2002, **11**, 125; (*c*) M. Yamanaka, K. Hara and J. Kudo, *Appl. Environ. Microbiol.*, 2005, **71**, 7589.
3 (*a*) B. Gole, A. K. Bar and P. S. Mukherjee, *Chem. Commun.*, 2011, **47**, 12137; (*b*) J. Aguilera-Sigalat and D. Bradshaw, *Chem. Commun.*, 2014, **50**, 4711; (*c*) K. P. Carter, A. M. Young and A. E. Palmer, *Chem. Rev.*, 2014, **114**, 4564; (*d*) K. Jayaramulu, R. P. Narayanan, S. J. George and T. K. Maji, *Inorg.Chem.*, 2012, **51**, 10089; (*e*) J. H. Wang, M. Li and D. Li, *Chem. Sci.*, 2013, **4**, 1793. (*f*) M. M. Wanderley, C. Wang, C. D. Wu and W. B. Lin, *J. Am. Chem. Soc.*, 2012, **134**, 9050.
4 (*a*) L. J. Li, S. F. Tang, C. Wang, X. X. Lv, M. Jiang, H. Z. Wu and X. B. Zhao, *Chem. Commun.*, 2014, **50**, 2304; (*b*) F. Gándara, H. Furukawa, S. Lee and O. M. Yaghi, *J. Am. Chem. Soc.*, 2014, **136**, 5271; (*c*) Y. L. Wang, C. H. Tan, Z. H. Sun, Z. Z. Xue, Q. L. Zhu, C. J. Shen, Y. H. Wen, S. M. Hu, Y. Wang, T. L. Sheng and X. T. Wu, *Chem. Eur. J.*, 2014, **20**, 1341; (d) Y. B. He, W. Zhou, G. D. Qian and B. L. Chen, *Chem. Soc. Rev.*, 2014, **43**, 5657.
5 (*a*) S. L. Qiu, M. Xue and G. S. Zhu, *Chem. Soc. Rev.*, 2014, **43**, 6116; (*b*) H. M. Yin, J. Q. Wang, Z. Xie, J. H. Yang, J. Bai, J. M. Lu, Y. Zhang, D. H. Yin and J. Y. S. Lin, *Chem. Commun.*,2014, **50**, 3699; (*c*) Z. Z. Xie, T. Li, N. L. Rosi and M. A. Carreon, *J. Mater. Chem. A.*,2014, **2**, 1239; (*d*) T. Rodenas, M. van Dalen, E. García-Pérez, P. Serra-Crespo, B. Zornoza, F. Kapteijn and J. Gascon, *Adv. Funct. Mater.*, 2014, **24**, 249.
6 (*a*) O. Kozachuk, I. Luz, F. X. L. Xamena, H. Noei, M. Kauer, H. B. Albada, E. D. Bloch, B. Marler, Y. M. Wang, M. Muhler and R. A. Fischer, *Angew. Chem. Int. Ed.*, 2014, **53**, 1; (*b*) K. Manna, T. Zhang and W. B. Lin, *J. Am. Chem. Soc.*, 2014, **136**, 6566; (*c*) M. Yoon, R. Srirambalaji and K. Kim, *Chem. Rev.*, 2011, **112**, 1196.
7 (*a*) Z. M. Hao, X. Z. Song, M. Zhu, X. Meng, S. N. Zhao, S. Q. Su, W. T. Yang, S. Y. Song and H. J. Zhang, *J. Mater. Chem. A.*, 2013, **1**, 11043; (*b*) L. E. Kreno, K. Leong, O. K. Farha, M. Allendorf, R. P. Van Duyne and J. T. Hupp, *Chem. Rev.*, 2012, **112**, 1105; (*c*) D. X. Ma, B. Y. Li, X. J. Zhou, Q. Zhou, K. Liu, G. Zeng, G. H. Li, Z. Shi and S. H. Feng, *Chem. Commun.*, 2013, **49**, 8964; (*d*) M. Zhang, G. Feng, Z. G. Song, Y. P. Zhou, H. Y. Chao, D. Q. Yuan, T. T. Y. Tan, Z. G. Guo, Z. G. Hu, B. Z. Tang, B. Liu and D. Zhao, *J. Am. Chem. Soc.*, 2014, **136**, 7241.
8 (*a*) Z. C. Hu, B. J. Deibert and J. Li, *Chem. Soc. Rev.*, 2014, **43**, 5815; (*b*) S. S. Nagarkar, B. Joarder, A. K. Chaudhari, S. Mukherjee and S. K. Ghosh, *Angew. Chem.*, 2013, **125**, 2953; (*c*) Z. H. Xiang, C. Q. Fang, S. H. Leng and D. P. Cao, *J. Mater. Chem. A.*, 2014, **2**, 7662; (*d*) M. D. Alledorf, C. A. Bauer, R. K. Bhakta and R. J. T. Houk, *Chem. Soc. Rev.*, 2009, **38**, 1330.
9 (*a*) H. H. Li, W. Shi, K. N. Zhao, Z. Niu, H. M. Li and P. Cheng, *Chem. Eur. J.*, 2013, **19**, 3358; (*b*) H. Liu, X. F. Peng and H. P. Zeng, *Inorg. Chem. Commun.*, 2014, **46**, 39; (*c*) M. L. Ma, C. Ji and S. Q. Zang, *Dalton Trans.*, 2013, **42**, 10579.
10 (*a*) J. M. Zhou, W. Shi, H. M. Li, H. Li and P. Cheng, *J. Phys. Chem. C.*, 2014, **118**, 416; (*b*) M. Zheng, H. Q. Tan, Z. G. Xie, L. G. Zhang, X. B.

Jing and Z. C. Sun, *ACS Appl. Mater. Interfaces.*, 2013, **5**, 1078; (*c*) Z. Chen, Y. W. Sun, L. L. Zhang, D. Sun, F. L. Liu, Q. G. Meng, R. M. Wang and D. F. Sun, *Chem. Commun.*, 2013, **49**, 11557; (*d*) J. M. Zhou, W. Shi, N. Xu and P. Cheng, *Inorg. Chem.*, 2013, **52**, 8082; (*e*) Y. M. Zhu, C. H. Zeng, T. S. Chu, H. M. Wang, Y. Y. Yang, Y. X. Tong, C. Y. Su and W. T. Wong, *J. Mater. Chem. A.*, 2013, **1**, 11312; (*f*) M. C. Das, G. D. Qian and B. L. Chen, *Chem. Commun.*, 2011, **47**, 11715; (*g*) R. Wang, X. Y. Dong, H. Xu, R. B. Pei, M. L. Ma, S. Q. Zang, H. W. Hou and T. C. W. Mak, *Chem. Commun.*, 2014, **50**, 9153.

11 (*a*) R. Decadt, K. Van Hecke, D. Depla, K. Leus, D. Weinberger, I. Van Driessche, P. Van der Voort and R. Van Deun, *Inorg. Chem.*, 2012, **51**, 11623; (*b*) M. Ji, X. Lan, Z. P. Han, C. Hao and J. S. Qiu, *Inorg. Chem.*, 2012, **51**, 12389.

12 S. M. Cohen, *Chem. Rev.*, 2012, **112**, 970.

13 J. An, C. M. Shade, D. A. Chengelis-Czegan, S. Petoud and N. L. Rosi, *J. Am. Chem. Soc.*, 2011, **133**, 1220.

14 M. L. Ma, J. H. Qin, C. Ji, H. Xu, R. Wang, B. J. Li, S. Q. Zang, H. W. Hou and S. R. Batten, *J. Mater. Chem. C.*, 2014, **2**, 1085.

15 Y. Y. Liu, R. Decadt, T. Bogaerts, K. Hemelsoet, A. M. Kaczmarek, D. Poelman, M. Waroquier, V. Van Speybroeck, R. Van Deun and P. Van Der Voort, *J. Phys. Chem. C.*, 2013, **117**, 11302.

16 J. W. Cao, Y. F. Gao, Y. Q. Wang, C. F. Du and Z. L. Liu, *Chem. Commun.,* 2013, **49**, 6897.

17 Y. Zhou and B. Yan, *Inorg. Chem.*, 2014, **53**, 3456.

18 C. Volkringer, T. Loiseau, N. Guillou, G. Ferey, M. Haouas, F. Taulelle, E. Elkaim and N. Stock, *Inorg. Chem.*, 2010, 49, 9852.

19 T. Loiseau, C. Serre, C. Huguenard, G. Fink, F. Taulelle, M. Henry,T. Bataille and G. Fÿrey, *Chem. Eur. J.*, 2004, **10**, 1373.

20 (a) B. R. Judd, *Phys. Rev.*, 1962, **127**, 750; (*b*) Y. Zhou, B. Yan and X. H. He, *J. Mater. Chem. C*, 2014, **2**, 848.

21 U. S. EPA, Ambient water quality criteria for silver, EPA 440-5-80-071, Final/Technical Report, Washington, DC, 1980.

22 N. Arnaud, E. Vaquer and J. Georges, *Analyst*, 1998, **123**, 261

23 (*a*) H. L. Tan and Y. Chen, *Chem. Commun.*, 2011, **47**, 12373; (*b*) Q. Tang, S. X. Liu, Y. W. Liu, J. Miao, S. J. Li, L. Zhang, Z. Shi and Z. P. Zheng, *Inorg. Chem.* 2013, **52**, 2799; (*c*) B. Zhao, X. Chen,P. Cheng, D. Liao, S. Yan and Z. Jiang, *J. Am. Chem. Soc.*, 2004, **126**, 15394; (*d*) K. Hanaoka, K. Kikuchi, H. Kojima, Y. Urano and T. Nagano, *J. Am. Chem. Soc.*, 2004, **126**, 12470; (*e*) K. Hanaoka, K. Kikuchi, H. Kojima, Y. Urano and T. Nagano, *Angew. Chem., Int. Ed.*, 2003, **42**, 2996; (*f*) C. F. De Sá, O. L. Malta, C. A. De Mello Donegá, M. Simas, R. L. Longo, P. A. Santa-Cruz and E. F. da Silva, *Jr. Coord. Chem. Rev*. 2000, ***196***, 165; (*g*) S. I. Klink, H. Keizer and F. C. J. M. van Veggel, *Angew.Chem. Int. Ed.*, 2000, **39**, 4319; (*h*) A. Heller and E. Wasserman, *J. Chem. Phys.*, 1965, **42**, 949.